

RECOMMENDATION ITU-R P.452-8

PREDICTION PROCEDURE FOR THE EVALUATION OF MICROWAVE INTERFERENCE BETWEEN STATIONS ON THE SURFACE OF THE EARTH AT FREQUENCIES ABOVE ABOUT 0.7 GHz*

(Question ITU-R 208/3)

(1970-1974-1978-1982-1986-1992-1994-1995-1997)

The ITU Radiocommunication Assembly,

considering

- a) that due to congestion of the radio spectrum, frequency bands must be shared between different terrestrial services, between systems in the same service and between systems in the terrestrial and Earth-space services;
- b) that for the satisfactory coexistence of systems sharing the same frequency bands, interference propagation prediction procedures are needed that are accurate and reliable in operation and acceptable to all parties concerned;
- c) that interference propagation predictions are required to meet “worst-month” performance and availability objectives;
- d) that prediction methods are required for application to all types of path in all areas of the world,

recommends

1 that the microwave interference prediction procedure given in Annex 1 be used for the evaluation of the available propagation loss in interference calculations between stations on the surface of the Earth for frequencies above about 0.7 GHz.

ANNEX 1

1 Introduction

Congestion of the radio-frequency spectrum has made necessary the sharing of many frequency bands between different radio services, and between the different operators of similar radio services. In order to ensure the satisfactory coexistence of the terrestrial and Earth-space systems involved, it is important to be able to predict with reasonable accuracy the interference potential between them, using prediction procedures and models which are acceptable to all parties concerned, and which have demonstrated accuracy and reliability.

Many types and combinations of interference path may exist between stations on the surface of the Earth, and between these stations and stations in space, and prediction methods are required for each situation. This Annex addresses one of the more important sets of interference problems, i.e. those situations where there is a potential for interference between microwave radio stations located on the surface of the Earth.

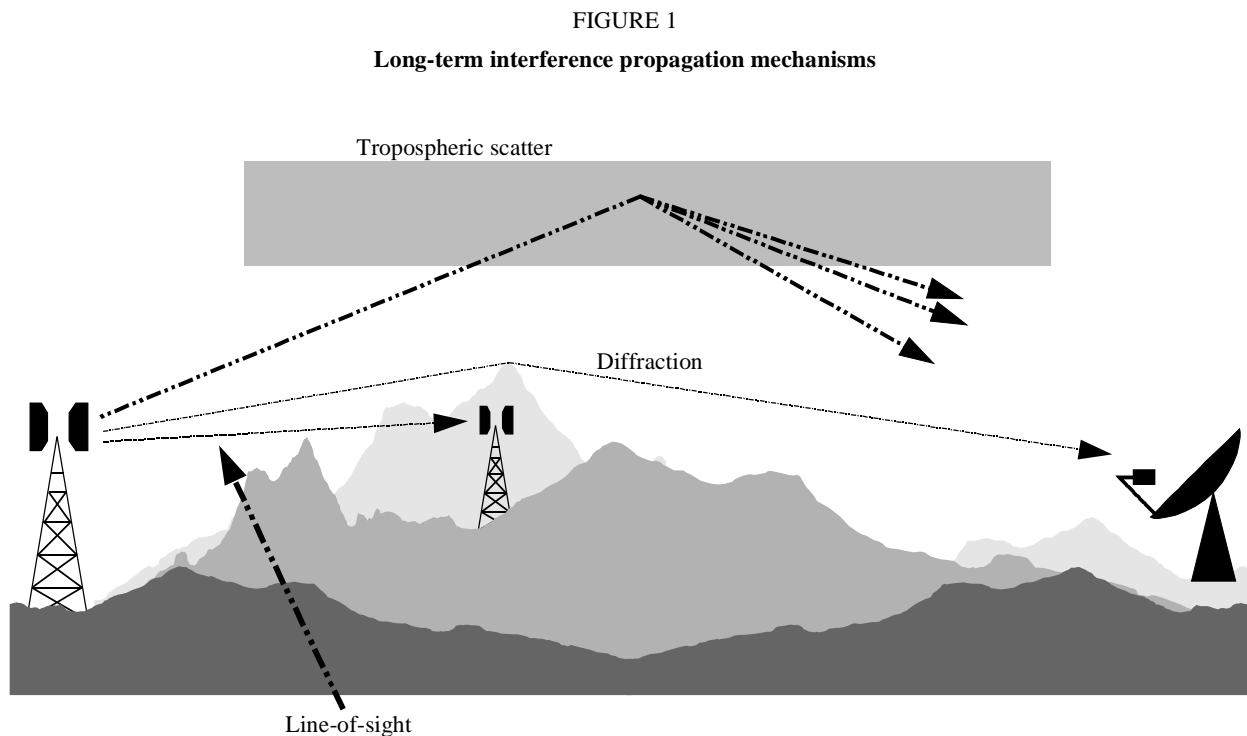
The prediction procedure is appropriate to radio stations operating in the frequency range of about 0.7 GHz to 30 GHz. The method includes a complementary set of propagation models which ensure that the predictions embrace all the significant interference propagation mechanisms that can arise. Methods for analysing the radio-meteorological and topographical features of the path are provided so that predictions can be prepared for any practical interference path falling within the scope of the procedure.

* Computer programs (REC452 and SCAT) associated with prediction procedures described in this Recommendation are available from the ITU; for details, see the ITU Radiocommunication Bureau (BR) Catalogue of Software for Radio Spectrum Management.

2 Interference propagation mechanisms

Microwave interference may arise through a range of propagation mechanisms whose individual dominance depends on climate, radio frequency, time percentage of interest, distance and path topography. At any one time a single mechanism or more than one may be present. The principal interference propagation mechanisms are as follows:

- *Line-of-sight* (Fig. 1): The most straightforward interference propagation situation is when a line-of-sight transmission path exists under normal (i.e. well-mixed) atmospheric conditions. However, an additional complexity can come into play when subpath diffraction causes a slight increase in signal level above that normally expected. Also, on all but the shortest paths (i.e. paths longer than about 5 km) signal levels can often be significantly enhanced for short periods of time by multipath and focusing effects resulting from atmospheric stratification (see Fig. 2).
- *Diffraction* (Fig. 1): Beyond line-of-sight and under normal conditions, diffraction effects generally dominate wherever significant signal levels are to be found. For services where anomalous short-term problems are not important, the accuracy to which diffraction can be modelled generally determines the density of systems that can be achieved. The diffraction prediction capability must have sufficient utility to cover smooth-Earth, discrete obstacle and irregular (unstructured) terrain situations.
- *Tropospheric scatter* (Fig. 1): This mechanism defines the «background» interference level for longer paths (e.g. more than 100-150 km) where the diffraction field becomes very weak. However, except for a few special cases involving sensitive earth stations or very high power interferers (e.g. radar systems), interference via troposcatter will be at too low a level to be significant.

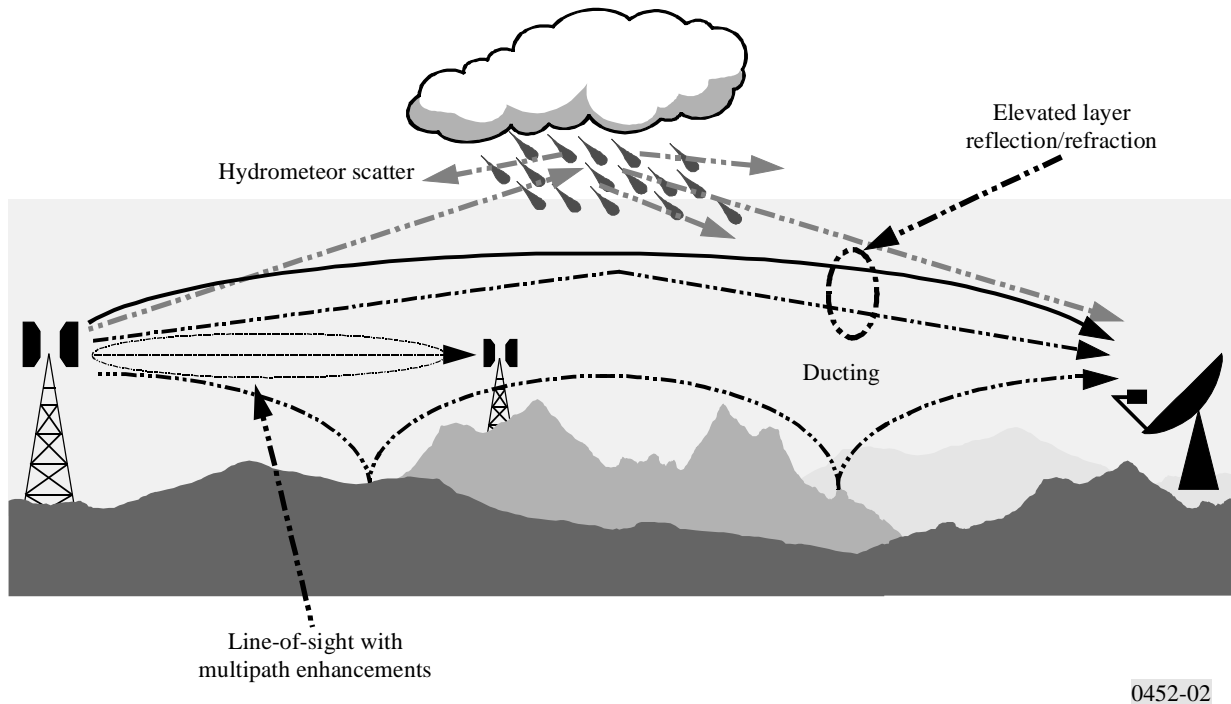


0452-01

- *Surface ducting* (Fig. 2): This is the most important short-term interference mechanism over water and in flat coastal land areas, and can give rise to high signal levels over long distances (more than 500 km over the sea). Such signals can exceed the equivalent “free-space” level under certain conditions.
- *Elevated layer reflection and refraction* (Fig. 2): The treatment of reflection and/or refraction from layers at heights up to a few hundred metres is of major importance as these mechanisms enable signals to overcome the diffraction loss of the terrain very effectively under favourable path geometry situations. Again the impact can be significant over quite long distances (up to 250-300 km).

- *Hydrometeor scatter* (Fig. 2): Hydrometeor scatter can be a potential source of interference between terrestrial link transmitters and earth stations because it may act virtually omnidirectionally, and can therefore have an impact off the great-circle interference path. However, the interfering signal levels are quite low and do not usually represent a significant problem.

FIGURE 2
Anomalous (short-term) interference propagation mechanisms



A basic problem in interference prediction (which is indeed common to all tropospheric prediction procedures) is the difficulty of providing a unified consistent set of practical methods covering a wide range of distances and time percentages; i.e. for the real atmosphere in which the statistics of dominance by one mechanism merge gradually into another as meteorological and/or path conditions change. Especially in these transitional regions, a given level of signal may occur for a total time percentage which is the sum of those in different mechanisms. The approach in this procedure has been deliberately to keep separate the prediction of interference levels from the different propagation mechanisms up to the point where they can be combined into an overall prediction for the path.

3 Clear-air interference prediction

3.1 General comments

The procedure uses five propagation models to deal with the clear-air propagation mechanisms described in § 2 above. These models are as follows:

- *line-of-sight* (including signal enhancements due to multipath and focusing effects);
- *diffraction* (embracing smooth-Earth, irregular terrain and sub-path cases);
- *tropospheric scatter*;
- *anomalous propagation* (ducting and layer reflection/refraction);
- *height-gain variation in clutter* (where relevant).

Depending on the type of path, as determined by a path profile analysis, one or more of these models are exercised in order to provide the required prediction of basic transmission loss.

3.2 Deriving a prediction

3.2.1 Outline of the procedure

The steps required to achieve a prediction are as follows:

Step 1: Input data

The basic input data required for the procedure is given in Table 1. All other information required is derived from these basic data during the execution of the procedure.

TABLE 1
Basic input data

| Parameter | Preferred resolution | Description |
|------------------|----------------------|--|
| f | 0.01 | Frequency (GHz) |
| p | 0.001 | Required time percentage(s) for which the calculated basic transmission loss is not exceeded |
| Φ_t, Φ_r | 0.001 | Latitude of station (degrees) |
| Ψ_t, Ψ_r | 0.001 | Longitude of station (degrees) |
| h_{tg}, h_{rg} | 1 | Antenna centre height above ground level (m) |
| h_{ts}, h_{rs} | 1 | Antenna centre height above mean sea level (m) |
| G_t, G_r | 0.1 | Antenna gain in the direction of the horizon along the great-circle interference path (dBi) |

NOTE 1 – For the interfering and interfered-with stations:

t : interferer

r : interfered-with station.

Step 2: Selecting average year or worst-month prediction

The choice of annual or “worst-month” predictions is generally dictated by the quality (i.e. performance and availability) objectives of the interfered-with radio system at the receiving end of the interference path. As interference is often a bidirectional problem, two such sets of quality objectives may need to be evaluated in order to determine the worst-case direction upon which the minimum permissible basic transmission loss needs to be based. In the majority of cases the quality objectives will be couched in terms of a percentage “of any month”, and hence worst-month data will be needed.

The propagation prediction models predict the annual distribution of basic transmission loss. For average year predictions the percentages of time p , for which particular values of basic transmission loss are not exceeded, are used directly in the prediction procedure. If average worst-month predictions are required, the annual equivalent time percentage, p , of the worst-month time percentage, p_w , must be calculated for the path centre latitude ϕ using:

$$p = \frac{p_w}{Q} \quad \% \quad (1)$$

where:

$$Q = \frac{0.85 \times 10^{(0.078 \omega - 0.184) \log p + 0.186 \omega + 0.515}}{G_L} \quad (1a)$$

where:

ω : fraction of the path over water (see Table 3).

The value of Q must be limited to $Q \leq 12$:

$$G_L = \begin{cases} \sqrt{1.1 + |\cos 2 \varphi|^{0.7}} & \text{for } |\varphi| \leq 45^\circ \\ \sqrt{1.1 - |\cos 2 \varphi|^{0.7}} & \text{for } |\varphi| > 45^\circ \end{cases} \quad (1b)$$

Note that the latitude φ (degrees) is deemed to be positive in the Northern Hemisphere.

The calculated result will then represent the basic transmission loss for the required worst-month time percentage, $p_w\%$.

Step 3: Radiometeorological data

The prediction procedure employs three radio-meteorological parameters to describe the variability of background and anomalous propagation conditions at the different locations around the world.

- ΔN (N-units/km), the average radio-refractive index lapse-rate through the lowest 1 km of the atmosphere, provides the data upon which the appropriate effective Earth radius can be calculated for path profile and diffraction obstacle analysis. Figures 4 and 5, respectively, provide world maps of average annual ΔN values and maximum monthly mean values for worst-month predictions. Note that ΔN is a positive quantity in this procedure.
- β_0 (%), the time percentage for which refractive index lapse-rates exceeding 100 N-units/km can be expected in the first 100 m of the lower atmosphere, is used to estimate the relative incidence of fully developed anomalous propagation at the latitude under consideration. The value of β_0 to be used is that appropriate to the path centre latitude.
- N_0 (N-units), the sea-level surface refractivity, is used only by the troposcatter model as a measure of location variability of the troposcatter scatter mechanism. Figure 6 provides annual values of N_0 . As the scatter path calculation is based on a path geometry determined by annual or worst-month values of ΔN , there is no additional need for worst-month values of N_0 . The correct values of ΔN and N_0 are given by the path-centre values as derived from the appropriate maps.

Point incidence of anomalous propagation, β_0 (%), for the path centre location is determined using:

$$\beta_0 = \begin{cases} 10^{-0.015|\varphi| + 1.67} \mu_1 \mu_4 \quad \% & \text{for } |\varphi| \leq 70^\circ \\ 4.17 \mu_1 \mu_4 \quad \% & \text{for } |\varphi| > 70^\circ \end{cases} \quad (2)$$

where:

φ : path centre latitude (degrees)

The parameter μ_1 depends on the degree to which the path is over land (inland and/or coastal) and water, and is given by:

$$\mu_1 = \left[10^{\frac{-d_{lm}}{16 - 6.6 \tau}} + \left[10^{-(0.496 + 0.354 \tau)} \right]^5 \right]^{0.2} \quad (3)$$

where the value of μ_1 shall be limited to $\mu_1 \leq 1$,

with:

$$\tau = \left[1 - e^{-\left(4.12 \times 10^{-4} \times d_{lm}^{2.41}\right)} \right] \quad (3a)$$

where:

d_{lm} : longest continuous land (inland + coastal) section of the great-circle path (km)

d_{lm} : longest continuous inland section of the great-circle path (km).

The radioclimatic zones to be used for the derivation of d_{lm} and d_{lm} are defined in Table 2.

$$\mu_4 = \begin{cases} 10^{(-0.935 + 0.0176|\varphi|)\log \mu_1} & \text{for } |\varphi| \leq 70^\circ \\ 10^{0.3 \log \mu_1} & \text{for } |\varphi| > 70^\circ \end{cases} \quad (4)$$

TABLE 2

Radio-climatic zones

| Zone type | Code | Definition |
|--------------|------|--|
| Coastal land | A1 | Coastal land and shore areas, i.e. land adjacent to the sea up to an altitude of 100 m relative to mean sea or water level, but limited to a distance of 50 km from the nearest sea area. Where precise 100 m data is not available an approximate value, i.e. 300 ft, may be used |
| Inland | A2 | All land, other than coastal and shore areas defined as "coastal land" above |
| Sea | B | Seas, oceans and other large bodies of water (i.e. covering a circle of at least 100 km in diameter) |

Large bodies of inland water

A "large" body of inland water, to be considered as lying in Zone B, is defined as one having an area of at least 7 800 km², but excluding the area of rivers. Islands within such bodies of water are to be included as water within the calculation of this area if they have elevations lower than 100 m above the mean water level for more than 90% of their area. Islands that do not meet these criteria should be classified as land for the purposes of the water area calculation.

Large inland lake or wet-land areas

Large inland areas of greater than 7 800 km² which contain many small lakes or a river network should be declared as "coastal" Zone A1 by administrations if the area comprises more than 50% water, and more than 90% of the land is less than 100 m above the mean water level.

Climatic regions pertaining to Zone A1, large inland bodies of water and large inland lake and wetland regions, are difficult to determine unambiguously. Therefore administrations are requested to register with the ITU BR those regions within their territorial boundaries that they wish identified as belonging to one of these categories. In the absence of registered information to the contrary, all land areas will be considered to pertain to climate Zone A2.

For maximum consistency of results between administrations it is strongly recommended that the calculations of this procedure be based on the ITU-R Digitized World Map (IDWM) which is available from the ITU (BR) for mainframe or personal computer environments

Effective Earth's radius

The median effective Earth radius factor k_{50} for the path is determined using:

$$k_{50} = \frac{157}{157 - \Delta N} \quad (5)$$

Assuming a true Earth radius of 6 371 km, the median value of effective Earth radius a_e can be determined from:

$$a_e = 6\,371 \cdot k_{50} \quad \text{km} \quad (6)$$

Step 4: Path profile analysis

Values for a number of path-related parameters necessary for the calculations, as indicated in Table 3, must be derived via an initial analysis of the path profile based on the value of a_e given by equation (6). Information on the derivation, construction and analysis of the path profile is given in Appendix 2. Having thus analysed the profile, the path will also have been classified into one of the three geometrical categories indicated in Table 4.

NOTE 1 – The determination of values for additional profile-related parameters required specifically for diffraction calculations is described in Recommendation ITU-R P.526.

TABLE 3

Parameter values to be derived from the path profile analysis

| Path type | Parameter | Description |
|---------------|----------------------|---|
| Trans-horizon | d | Great-circle path distance (km) |
| Trans-horizon | d_{lt}, d_{lr} | Distance from the transmit and receive antennas to their respective horizons (km) |
| Trans-horizon | θ_t, θ_r | Transmit and receive horizon elevation angles respectively (mrad) |
| Trans-horizon | θ | Path angular distance (mrad) |
| All | h_{ts}, h_{rs} | Antenna centre height above mean sea level (m) |
| Trans-horizon | h_{te}, h_{re} | Effective heights of antennas above the terrain (m) (see Appendix 2 for definitions) |
| All | $d_b^{(1)}$ | Aggregate length of the path sections over water (km) |
| All | $\omega^{(1)}$ | Fraction of the total path over water: $\omega = d_b/d \quad (7)$ where d is the great-circle distance (km) calculated using equation (34). For totally overland paths $\omega = 0$ |
| Trans-horizon | $d_{ct}^{(1)}$ | Distance from the first terminal (the interference source) to the coast along the great-circle interference path (km) |
| Trans-horizon | $d_{cr}^{(1)}$ | Corresponding distance for the second (interfered-with) station (km) |

⁽¹⁾ These parameters are only required when the path has one or more sections over water.

The exact values of d_{ct} and d_{cr} are only of importance if d_{ct} and $d_{cr} \leq 5$ km. If, in either or both cases, the distances are obviously in excess of 5 km, then it is only necessary to note the > 5 km condition. Few interference paths will in fact need detailed evaluation of these two parameters.

Step 5: Calculation of propagation predictions

Table 4 indicates, for each type of path, the propagation models that are appropriate. The necessary equations for these individual propagation mechanism predictions are to be found in the text sections indicated in the table. In order to build an overall prediction, the individual propagation mechanism predictions must be calculated and combined in the manner shown in Table 5. Once this has been achieved for each of the required time percentages, the prediction is complete.

TABLE 4

Interference path classifications and propagation model requirements

| Classification | Models required |
|---|--|
| Line-of-sight with first Fresnel zone clearance | Line-of-sight (§ 4.2) Clutter loss (§ 4.5, where appropriate) |
| Line-of-sight with sub-path diffraction, i.e. terrain incursion into the 1st Fresnel zone | Line-of-sight (§ 4.2) Diffraction (§ 4.3) Clutter loss (§ 4.3, where appropriate) |
| Trans-horizon | Diffraction (§ 4.3 for $d \leq 200$ km) Ducting/layer reflection (§ 4.5 for $d > 20$ km) Troposcatter (§ 4.4) Clutter loss (§ 4.5, where appropriate) |

TABLE 5

Methods of deriving overall predictions

| Path type | Action required |
|---|--|
| Line-of-sight | <p>The prediction is obtained by summing the losses given by the line-of-sight and clutter loss models, i.e.:</p> $L_b(p) = L_{b0}(p) + A_{ht} + A_{hr} \quad \text{dB} \quad (8a)$ <p>where:</p> <p>$L_{b0}(p)$: predicted basic transmission loss not exceeded for $p\%$ of time given by the line-of-sight model</p> <p>A_{ht}, A_{hr}: appropriate additional losses due to height-gain effects in local clutter</p> |
| Line-of-sight with sub-path diffraction | <p>The prediction is obtained by summing the losses given by the line-of-sight and (sub-path) diffraction models and clutter models, i.e.:</p> $L_b(p) = L_{b0}(p) + L_{ds}(p) + A_{ht} + A_{hr} \quad \text{dB} \quad (8b)$ <p>where:</p> <p>$L_{ds}(p)$: prediction for $p\%$ of time given by the <i>sub-path</i> diffraction loss element of the diffraction model</p> |
| Trans-horizon | <p>The overall prediction can be obtained by applying the following ancillary algorithm:</p> $L_b(p) = -5 \log \left(10^{-0.2L_{bs}} + 10^{-0.2L_{bd}} + 10^{-0.2L_{ba}} \right) + A_{ht} + A_{hr} \quad \text{dB} \quad (8c)$ <p>where $L_{bs}(p)$, $L_{bd}(p)$ and $L_{ba}(p)$: individual predicted basic transmission loss for $p\%$ of time given by the troposcatter, diffraction and ducting/layer reflection propagation models respectively.</p> <p>NOTE 1 – Where a model has not been proposed for a path (because the conditions given in Table 4 were not met), the appropriate term should be omitted from equation (8c).</p> |

4 Clear-air propagation models**4.1 General**

The procedure given above invokes one or more separate propagation models to provide the components of the overall prediction. These propagation models are provided in this section.

4.2 Line-of-sight propagation (including short-term effects)

The basic transmission loss $L_{b0}(p)$ not exceeded for time percentage, p %, due to line-of-sight propagation is given by:

$$L_{b0}(p) = 92.5 + 20 \log f + 20 \log d + E_s(p) + A_g \quad \text{dB} \quad (9)$$

where:

$E_s(p)$: correction for multipath and focusing effects:

$$E_s(p) = 2.6 (1 - e^{-d/10}) \log (p/50) \quad \text{dB} \quad (10)$$

A_g : total gaseous absorption (dB):

$$A_g = [\gamma_o + \gamma_w(\rho)]d \quad \text{dB} \quad (11)$$

where:

$\gamma_o, \gamma_w(\rho)$: specific attenuation due to dry air and water vapour, respectively, and are found from the equations in Recommendation ITU-R P.676

ρ : water vapour density:

$$\rho = 7.5 + 2.5 \omega \quad \text{g/m}^3 \quad (11a)$$

ω : fraction of the total path over water.

4.3 Diffraction

The time variability of the excess loss due to the diffraction mechanism is assumed to be the result of changes in bulk atmospheric radio refractivity lapse rate, i.e. as the time percentage p reduces, the effective Earth radius factor $k(p)$ is assumed to increase. This process is considered valid for $\beta_0 \leq p \leq 50\%$. For time percentages less than β_0 signal levels are dominated by anomalous propagation mechanisms rather than by the bulk refractivity characteristics of the atmosphere. Thus for values of p less than β_0 the value of $k(p)$ has the value $k(\beta_0)$.

The value of effective Earth radius to use in diffraction calculations is given by:

$$a(p) = 6371 \cdot k(p) \quad \text{km} \quad (12)$$

where:

p : may take the values 50 or β_0

$k(50\%)$: is given by equation (5)

$k(\beta_0) = 3$.

The excess diffraction loss $L_d(p)$ is computed by the method described in Recommendation ITU-R P.526 § 4.5, combined with a log-normal distribution of loss between 50% and β_0 as follows:

- for $p = 50\%$, $L_d(50\%)$ is computed using the method described in Recommendation ITU-R P.526 for the median effective Earth radius $a(50\%)$;
- for $p \leq \beta_0$, $L_d(\beta_0)$ is computed using the method described in Recommendation ITU-R P.526 for effective Earth radius $a(\beta_0)$;
- for $\beta_0 < p < 50\%$ $L_d(p)$ is given by:

$$L_d(p) = L_d(50\%) - F_i(p) [L_d(50\%) - L_d(\beta_0)] \quad (13)$$

where:

F_i : interpolation factor based on a log-normal distribution of diffraction loss over the range $\beta_0\% < p < 50\%$ given by:

$$F_i = I(p/100) / I(\beta_0/100) \quad (13a)$$

where $I(x)$ is the inverse cumulative normal function. A suitable approximation for $I(x)$ which may be used with confidence for $x < 0.5$ is given in Appendix 4.

NOTE 1 – Recommendation ITU-R P.526 § 4.5 can be used for the calculation of diffraction loss over either a line-of-sight path with sub-path obstruction, or a trans-horizon path.

The basic transmission loss not exceeded for $p\%$ time for a diffraction path is then given by:

$$L_{bd}(p) = 92.5 + 20 \log f + 20 \log d + L_d(p) + E_{sd}(p) + A_g \quad \text{dB} \quad (14)$$

where:

$E_{sd}(p)$: correction for multipath effects between the antennas and the horizon obstacles.

$$E_{sd}(p) = 2.6 \left(1 - e^{-(d_t + d_{lr})/10} \right) \log \left(\frac{p}{50} \right) \quad \text{dB} \quad (14a)$$

A_g : gaseous absorption determined using equations (11) and (11a).

4.4 Tropospheric scatter (Notes 1 and 2)

NOTE 1 – At time percentages much below 50%, it is difficult to separate the true tropospheric scatter mode from other secondary propagation phenomena which give rise to similar propagation effects. The “tropospheric scatter” model adopted in this Recommendation is therefore an empirical generalization of the concept of tropospheric scatter which also embraces these secondary propagation effects. This allows a continuous consistent prediction of basic transmission loss over the range of time percentages p from 0.001% to 50%, thus linking the ducting and layer reflection model at the small time percentages with the true “scatter mode” appropriate to the weak residual field exceeded for the largest time percentage.

NOTE 2 – This troposcatter prediction model has been derived for interference prediction purposes and is not appropriate for the calculation of propagation conditions above 50% of time affecting the performance aspects of trans-horizon radio-relay systems.

The basic transmission loss due to troposcatter, $L_{bs}(p)$ (dB) not exceeded for any time percentage, p , below 50%, is given by:

$$L_{bs}(p) = 190 + L_f + 20 \log d + 0.573 \theta - 0.15 N_0 + L_c + A_g - 10.1 [-\log(p/50)]^{0.7} \quad \text{dB} \quad (15)$$

where:

L_f : frequency dependent loss:

$$L_f = 25 \log f - 2.5 [\log(f/2)]^2 \quad \text{dB} \quad (15a)$$

L_c : aperture to medium coupling loss (dB):

$$L_c = 0.051 \cdot e^{0.055(G_t + G_r)} \quad \text{dB} \quad (15b)$$

N_0 : path centre sea-level surface refractivity derived from Fig. 6

A_g : gaseous absorption derived from equation (11) using $\rho = 3 \text{ g/m}^3$ for the whole path length.

4.5 Ducting/layer reflection

The prediction of the basic transmission loss, $L_{ba}(p)$ (dB) occurring during periods of anomalous propagation (ducting and layer reflection) is based on the following function:

$$L_{ba}(p) = A_f + A_d(p) + A_g \quad \text{dB} \quad (16)$$

where:

A_f : total of fixed coupling losses (except for local clutter losses) between the antennas and the anomalous propagation structure within the atmosphere.

$$A_f = 102.45 + 20 \log f + 20 \log(d_{lt} + d_{lr}) + A_{st} + A_{sr} + A_{ct} + A_{cr} \quad \text{dB} \quad (17)$$

A_{st}, A_{sr} : site-shielding diffraction losses for the interfering and interfered-with stations respectively:

$$A_{st, sr} = \begin{cases} 20 \log \left[1 + 0.361 \theta''_{t,r} (f \cdot d_{lt,lr})^{1/2} \right] + 0.264 \theta''_{t,r} f^{1/3} & \text{dB for } \theta''_{t,r} > 0 \text{ mrad} \\ 0 & \text{dB for } \theta''_{t,r} \leq 0 \text{ mrad} \end{cases} \quad (18)$$

where:

$$\theta''_{t,r} = \theta_{t,r} - 0,1 d_{lt,lr} \quad \text{mrad} \quad (18a)$$

A_{ct}, A_{cr} : over-sea surface duct coupling corrections for the interfering and interfered-with stations respectively:

$$A_{ct, cr} = -3 e^{-0,25 d_{ct,cr}^2} \left[1 + \tanh (0.07(50 - h_{ts,rs})) \right] \quad \text{dB for } \omega \geq 0.75$$

$$d_{ct, cr} \leq d_{lt,lr} \quad (19)$$

$$d_{ct, cr} \leq 5 \text{ km}$$

$$A_{ct, cr} = 0 \quad \text{dB for all other conditions} \quad (19a)$$

It is useful to note the limited set of conditions under which equation (19) is needed.

$A_d(p)$: time percentage and angular-distance dependent losses within the anomalous propagation mechanism:

$$A_d(p) = \gamma_d \cdot \theta' + A(p) \quad \text{dB} \quad (20)$$

where:

γ_d : specific attenuation:

$$\gamma_d = 5 \times 10^{-5} a_e f^{1/3} \quad \text{dB/mrad} \quad (21)$$

θ' : angular distance (corrected where appropriate (via equation (22a)) to allow for the application of the site shielding model in equation (18)):

$$\theta' = \frac{10^3 d}{a_e} + \theta'_t + \theta'_r \quad \text{mrad} \quad (22)$$

$$\theta'_{t,r} = \begin{cases} \theta_{t,r} & \text{mrad for } \theta_{t,r} \leq 0.1 d_{lt,lr} \quad \text{mrad} \\ 0.1 d_{lt,lr} & \text{mrad for } \theta_{t,r} > 0.1 d_{lt,lr} \quad \text{mrad} \end{cases} \quad (22a)$$

$A(p)$: time percentage variability (cumulative distribution):

$$A(p) = -12 + (1.2 + 3.7 \times 10^{-3} d) \log \left(\frac{p}{\beta} \right) + 12 \left(\frac{p}{\beta} \right)^\Gamma \quad \text{dB} \quad (23)$$

$$\Gamma = \left[\frac{-1.079 + \log (142 - (1.2 + 3.7 \times 10^{-3} d) \cdot (2 - \log \beta))}{2 - \log \beta} \right] \quad (23a)$$

$$\beta = \beta_0 \cdot \mu_2 \cdot \mu_3 \quad \% \quad (24)$$

μ_2 : correction for path geometry:

$$\mu_2 = \left[\frac{500}{a_e} \frac{d^2}{(\sqrt{h_{te}} + \sqrt{h_{re}})^2} \right]^\alpha \quad (25)$$

The value of μ_2 shall not exceed 1.

$$\alpha = -0.6 - \varepsilon \cdot 10^{-9} \cdot d^{3.1} \cdot \tau \quad (25a)$$

where:

$$\varepsilon = 3.5$$

τ : is defined in equation (3a)

μ_3 : correction for terrain roughness:

$$\mu_3 = \begin{cases} 1 & \text{for } h_m \leq 10 \text{ m} \\ \exp \left[-4.6 \times 10^{-5} (h_m - 10) (43 + 6 d_i) \right] & \text{for } h_m > 10 \text{ m} \end{cases} \quad (26)$$

$$d_i = \min (d - d_{lt} - d_{lr}, 40) \quad \text{km} \quad (26a)$$

A_g : total gaseous absorption determined from equations (11) and (11a).

The remaining terms have been defined in Tables 1 and 2 and Appendix 2.

4.6 Additional clutter losses

4.6.1 General

Considerable benefit, in terms of protection from interference, can be derived from the additional diffraction losses available to antennas which are imbedded in local ground clutter (buildings, vegetation etc.). This procedure allows for the addition of such clutter losses at either or both ends of the path in situations where the clutter scenario is known. Where there are doubts as to the certainty of the clutter environment this additional loss should not be included.

The clutter losses are designated as A_{ht} (dB) and A_{hr} (dB) for the interferer and interfered-with stations respectively. The additional protection available is height dependent, and is therefore modelled by a height-gain function normalized to the nominal height of the clutter. Appropriate nominal heights are available for a range of clutter types.

The correction applies to all clear-air predictions in this Recommendation, i.e. for all propagation modes and time percentages.

4.6.2 Clutter categories

Table 6 indicates the clutter categories for which the height-gain correction can be applied. The nominal clutter height, h_a (m) and distance from the antenna, d_k (km) are deemed to be "average" values most representative of the clutter type. However, the correction model has been made conservative in recognition of the uncertainties over the actual height that are appropriate in individual situations. Where the clutter parameters are more accurately known they can be directly substituted for the values taken from Table 6.

4.6.3 The height-gain model

The additional loss due to protection from local clutter is given by the expression:

$$A_h = 10.25 \times e^{-d_k} \left(1 - \tanh \left[6 \left(\frac{h}{h_a} - 0.625 \right) \right] \right) - 0.33 \quad (27)$$

where:

d_k : distance (km) from nominal clutter point to the antenna (see Fig. 3)

h : antenna height (m) above local ground level

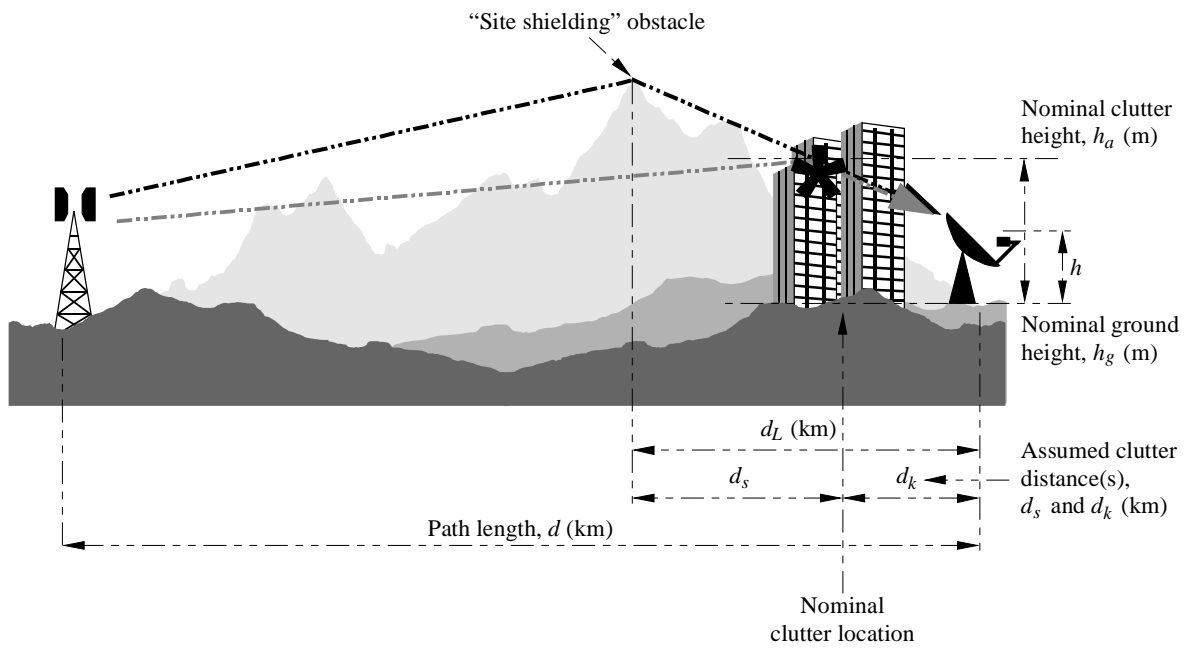
h_a : nominal clutter height (m) above local ground level.

TABLE 6

Nominal clutter heights and distances

| Category | Nominal height, h_a (m) | Nominal distance, d_k (km) |
|---|---------------------------|------------------------------|
| Open | 0 | -- |
| Rural (sparse vegetation and occasional isolated buildings) | 4 | 0.1 |
| Coniferous trees | 20 | 0.05 |
| Deciduous trees | 15 | 0.05 |
| Suburban | 9 | 0.025 |
| Urban | 20 | 0.02 |
| Dense urban | 25 | 0.02 |

FIGURE 3
Method of applying height-gain correction, A_{ht} or A_{hr}



4.6.4 Method of application

The method of applying the height-gain correction, A_{ht} or A_{hr} (dB) is straightforward, and is shown in Fig. 3.

The steps to be added to the basic prediction procedure are as follows:

Step 1: where the clutter type is known or can be safely assumed, the main procedure is used to calculate the basic transmission loss to the nominal height, h_a , for the appropriate clutter type, as selected from Table 6. The path length to be used is $d - d_k$ (km). However where $d \gg d_k$ this minor correction for d_k can safely be ignored.

Step 2: where there is a “site-shielding” obstacle that will provide protection to the terminal this should still be included in the basic calculation, but the shielding loss (A_{st} or A_{sr} (dB)) should be calculated to the height h_a at distance d_s , rather than to h at d_L as would otherwise be the case.

Step 3: once the main procedure is complete, the height gain correction from equation (27) can be added, as indicated in Table 5.

Step 4: where information on the clutter is not available, the basic calculation should be undertaken using distances d and d_L (if appropriate) and height h .

NOTE 1 – Clutter height-gain corrections should be added to both ends of the path where this is appropriate.

NOTE 2 – Where both the land height-gain correction and the sea duct coupling correction (A_{ct} or A_{cr} (dB)) are required (i.e. the antenna is close to the sea but there is intervening clutter), the two corrections can be used together as they are complementary and compatible.

NOTE 3 – If d is not significantly greater than d_k this model is not suitable.

5 Hydrometeor-scatter interference prediction

5.1 Introduction

This model, for which software (SCAT) is available from the ITU, predicts transmission loss statistics of an interfering signal from rainfall rate statistics. It is based on two fundamental assumptions:

- scattering occurs only within rain cells having circular cross-sections whose diameters depend on the rainfall rates inside the cell. For any link geometry, one cell is assumed to be in a fixed position which is intended to represent the worst case. Within the rain cell, the rainfall rate, and hence the reflectivity, is constant up to a rain height whose mean value depends on geographic latitude, but with a specific distribution about this mean that reflects the annual variation in height. Above the rain height, a linear decrease of the reflectivity (dB) is assumed;
- attenuation occurs inside as well as outside the cell, but only below the rain height. Inside the cell, the well known dependence of specific attenuation on the rainfall rate is assumed.

The model is able to compute interference levels for both long-path (> 100 km) and short-path geometries (down to a few kilometres) with arbitrary elevation angles at both terminals, as well as side scatter (non great-circle) geometries, and side-lobe coupling. Because of the complexity of the path geometry, it is available in the form of an example computer implementation.

The physical basis of the method is given in Appendix 3, where the intersection of a narrow beam (e.g., an earth station), and a wide beam (e.g., a terrestrial station) is assumed.

In comparative testing against both direct and radar-derived measurements, the method has yielded good results for a variety of frequencies and geometries.

5.2 Transmission loss formula

The transmission loss, L (dB), due to hydrometeor scatter, for a given rainfall rate, R , and rain height, h_{FR} , may be expressed as follows:

$$L = 197 - 10 \log \eta_E + 20 \log d_T - 20 \log f - 10 \log z_R + 10 \log S + A_g - 10 \log C \quad \text{dB} \quad (28)$$

where:

η_E : antenna efficiency (factor < 1) of the “earth” station

d_T : distance between stations via the scattering volume (km)

f : frequency (GHz)

z_R : unit volume rain scatter reflectivity factor below the (top of) rain height, h_{FR} (mm^6/m^3):

$$z_R = 400 R(p)^{1.4} \quad \text{mm}^6/\text{m}^3 \quad (29)$$

$R(p)$: point rainfall rate exceeded for time percentage, p , of interest

S : allowance for the deviation from Rayleigh law scattering in rain at frequencies above 10 GHz (assume $S = 0$ above h_{FR}):

$$10 \log S = R(p)^{0.4} \times 10^{-3} \left[4 (f - 10)^{1.6} \left(\frac{1 + \cos \varphi_s}{2} \right) + 5 (f - 10)^{1.7} \left(\frac{1 - \cos \varphi_s}{2} \right) \right] \quad \text{dB} \quad \text{for } f > 10 \text{ GHz} \quad (30a)$$

$$10 \log S = 0 \quad \text{dB} \quad \text{for } f \leq 10 \text{ GHz} \quad (30b)$$

φ_s : scatter angle, i.e. angle between the directions of propagation of the waves incident on, and outgoing from, the scatter volume (for example, $\varphi_s = 0^\circ$ for forward scatter, and $\varphi_s = 180^\circ$ for back scatter)

A_g : gaseous attenuation by oxygen and water vapour, calculated using the formulae of Recommendation ITU-R P.676 and a water vapour density of 7.5 g/m^3

C : effective scatter transfer function:

$$C = g_{T0} \int_{h_{min}}^{h_{max}} g_T(h) \zeta(h) A_T(h) A_E(h) \frac{1}{\sin \varepsilon_E} dh \quad (31)$$

where:

h_{min}, h_{max} : minimum and maximum heights for integration

g_{T0} : on-axis antenna gain factor of the terrestrial station

g_T : antenna directivity (factor ≤ 1) of the terrestrial station in the direction towards the integration point (volume element) under consideration

ε_E : elevation angle of earth station beam

$\zeta(h)$: reflectivity function in the scatter volume, normalized to z_R (the value below h_{FR})

$$\zeta(h) = 1 \quad \text{for } h \leq h_{FR} \quad (32a)$$

$$\zeta(h) = 10^{-0.65(h - h_{FR})} \quad \text{for } h > h_{FR} \quad (32b)$$

A_T, A_E : rain attenuation (factors ≤ 1) for the paths from the terrestrial station to the integration point and from there to the earth station, respectively. Information given in Appendix 3 is necessary for the calculation of A_T and A_E .

Equation (28) assumes the worst case (maximum) polarization coupling. For less than this ideal coupling, additional loss will occur (see Appendix 3).

To calculate the overall transmission loss, the integration of equation (31) has to be performed along the part of the earth station's antenna beam that is either, within the rain cell, or within the antenna beam of the terrestrial station (shown dark on Fig. 9).

The antenna beam of the terrestrial station is assumed to have a Gaussian shape. The integration is extended to the -18 dB points of the antenna pattern, relative to the maximum gain found along the narrow beam. To derive an analytical expression for the integral, the directivity pattern of the antenna of T is approximated by a Gaussian function as follows:

$$g_T(h) = \exp \left[-4 \ln 2 \left(\frac{h - h_0}{\Delta h_{1/2}} \right)^2 \right] \quad (33)$$

where $\Delta h_{1/2}$ is the difference of the heights of those two points on the antenna axis of the earth station where the directivity function of the antenna of the terrestrial station falls to 0.5 (-3 dB points).

5.3 Cumulative distribution of transmission loss

The (annual) cumulative distribution of transmission loss due to hydrometeor scatter is evaluated in two steps.

Firstly, for each combination of rainfall rate and rain height, the transmission loss is calculated as if there were a deterministic dependence on these parameters. It is assumed that this value of transmission loss happens with the same probability as the corresponding combination of rainfall rate and rain height, assuming statistical independence of these two parameters.

Secondly, the probabilities of all rainfall-rate/rain-height combinations leading to the same transmission loss values are summed to yield the total probability for that transmission loss. The resulting cumulative distribution is taken as the predicted distribution although there is no one-to-one correlation between the individual rainfall-rate/rain-height combinations and the transmission loss.

5.4 Worst-month predictions

Worst-month scaling factors, Q , for hydrometeor scatter have been found to be about 3 at 1% time, 4.5 at 0.01% time and about 7 at 0.001% time in Europe. These are based on a limited amount of data at frequencies of 11 GHz and above, and should be used prudently. It was found that the mean values were very close to the European rainfall rate factors. Therefore, in the absence of measured Q values for precipitation scatter, it is suggested that the Q values for rainfall rate be used instead (see Recommendation ITU-R P.841 for tables of Q values).

As an example, based on results for an 11 GHz path of 131 km in the United Kingdom, a transmission loss of 141 dB was exceeded for all but 0.01% of time on an annual basis. Using a Q factor of 4.5, the transmission loss exceeded for all but 0.002% of the annual distribution, 139.3 dB, would occur for 0.01% of the worst-month, a decrease in loss of 1.7 dB.

In principle, these worst-month factors should take complete account of the melting layer, but model calculations have suggested that the interference effect of this layer may be significant if it is centred on the common volume of the intersecting main beams for a significant period of time during, for example, a "worst-month". The effect is frequency dependent, being more significant at lower frequencies, such as 4-6 GHz, and less so at high frequencies. The effect was observed on measurements on a 131 km path at 11.2 GHz (composite rain climate C, D, E) which indicated that the presence of the melting layer in the summer increased the interference level by about 2-3 dB at percentages of time between 0.1% and 0.01%, relative to the expected enhancement in the seasonal statistics in the absence of the melting layer. At 5 GHz, the scaled interference enhancement due to the presence of the melting layer would be 3-4 dB. Worst-month enhancements in interference resulting from the presence of the melting layer would be slightly larger than these worst-season enhancements.

APPENDIX 1
TO ANNEX 1

Radio-meteorological data required for the clear-air prediction procedure

1 Introduction

The clear-air prediction procedures rely on radio-meteorological data to provide the basic location variability for the predictions. These data are provided in the form of maps which are contained in this Appendix.

2 Maps of vertical variation of radio refractivity data

For the global procedure, the clear-air radio-meteorology of the path is characterized for the continuous (long-term) interference mechanisms by the average annual value of ΔN (the refractive index lapse-rate over the first 1 km of the atmosphere) and for the anomalous (short-term) mechanisms by the time percentage, $\beta_0\%$, for which the refractive gradient of the lower atmosphere is below -100 N-units/km. These parameters provide a reasonable basis upon which to model the clear-air propagation mechanisms described in § 2 of Annex 1. For some of these quantities, data are provided in this Appendix for annual and worst-month calculations:

- Figure 4 provides average year ΔN data;
- Figure 5 provides the associated “maximum monthly mean” ΔN contours;

FIGURE 4
Average annual values of ΔN

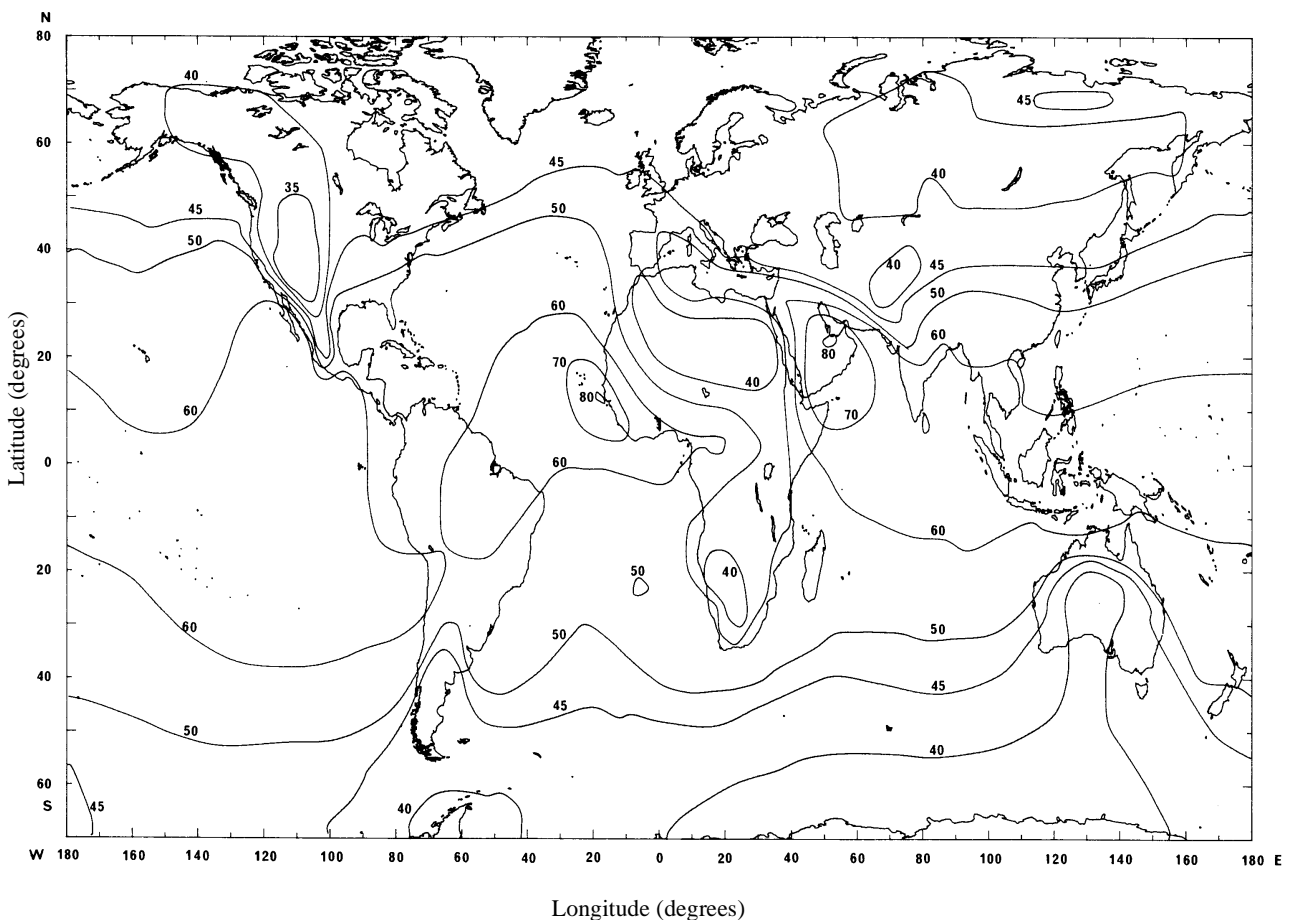
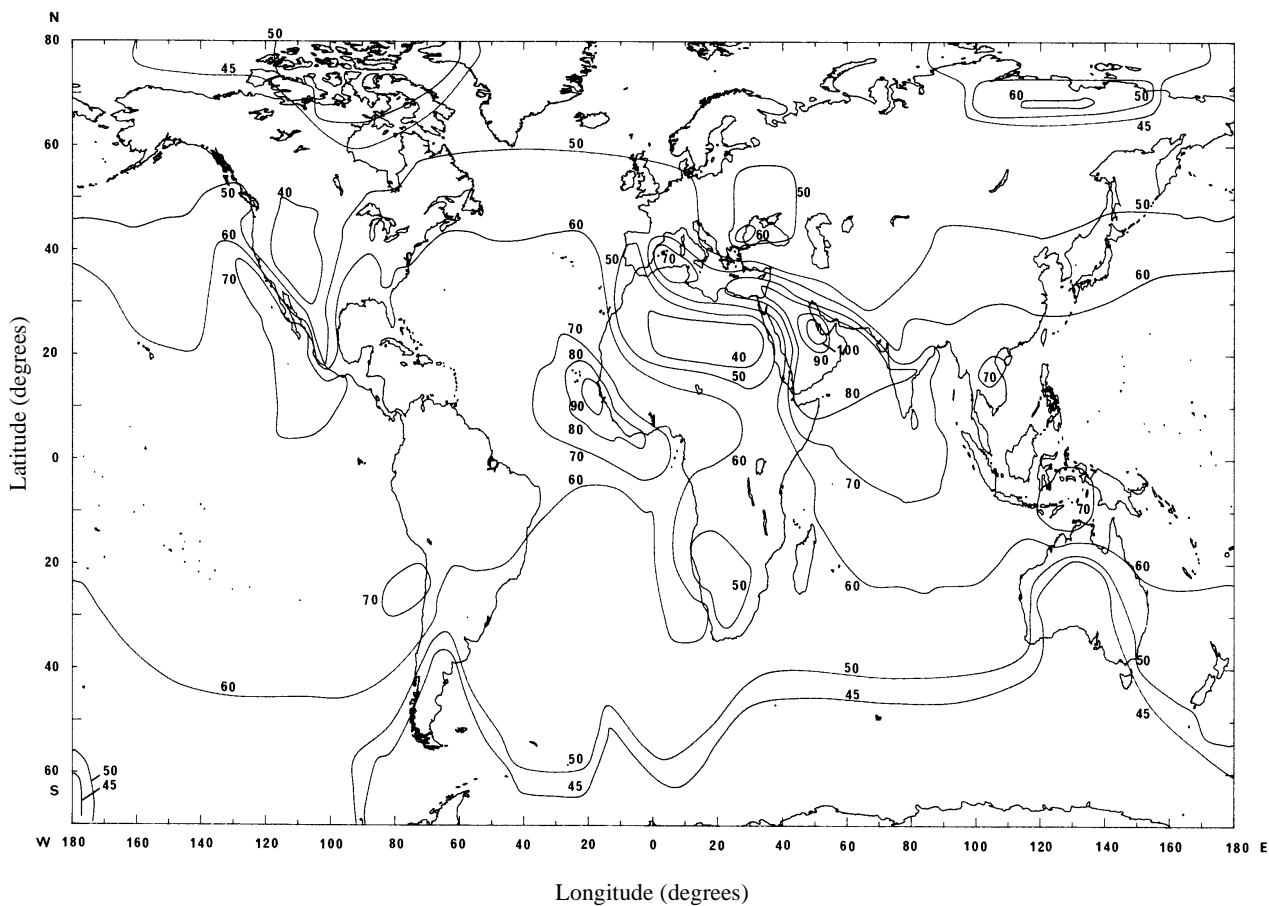


FIGURE 5
Maximum monthly mean values of ΔN (for worst-month prediction)

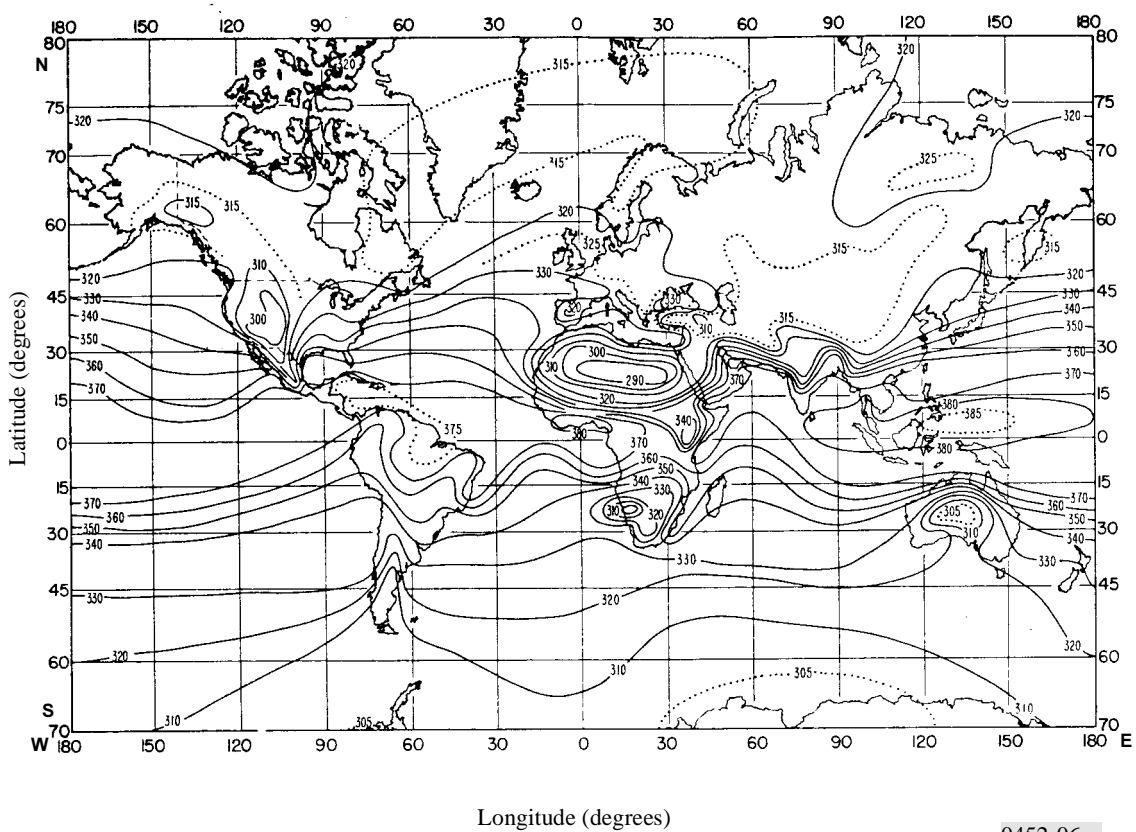


0452-05sc

3 Map of surface refractivity, N_0

Figure 6 provides a map of average sea-level surface refractivity, N_0 , for the troposcatter model.

FIGURE 6
Sea-level surface refractivity, N_0



0452-06sc

4 Implementation of maps in computer database form

For computer implementation of the procedures, it is convenient to capture these maps in digital form and to convert them into simple databases that can be accessed by the software.

For the global refractive index maps, it is suggested that the contours be converted into two-dimensional arrays of $0.5^\circ \times 0.5^\circ$ latitude and longitude. To avoid discontinuities in the prediction with small changes in location or distance the values for each array cell should be derived by interpolation between the contours.

APPENDIX 2
TO ANNEX 1

Path profile analysis

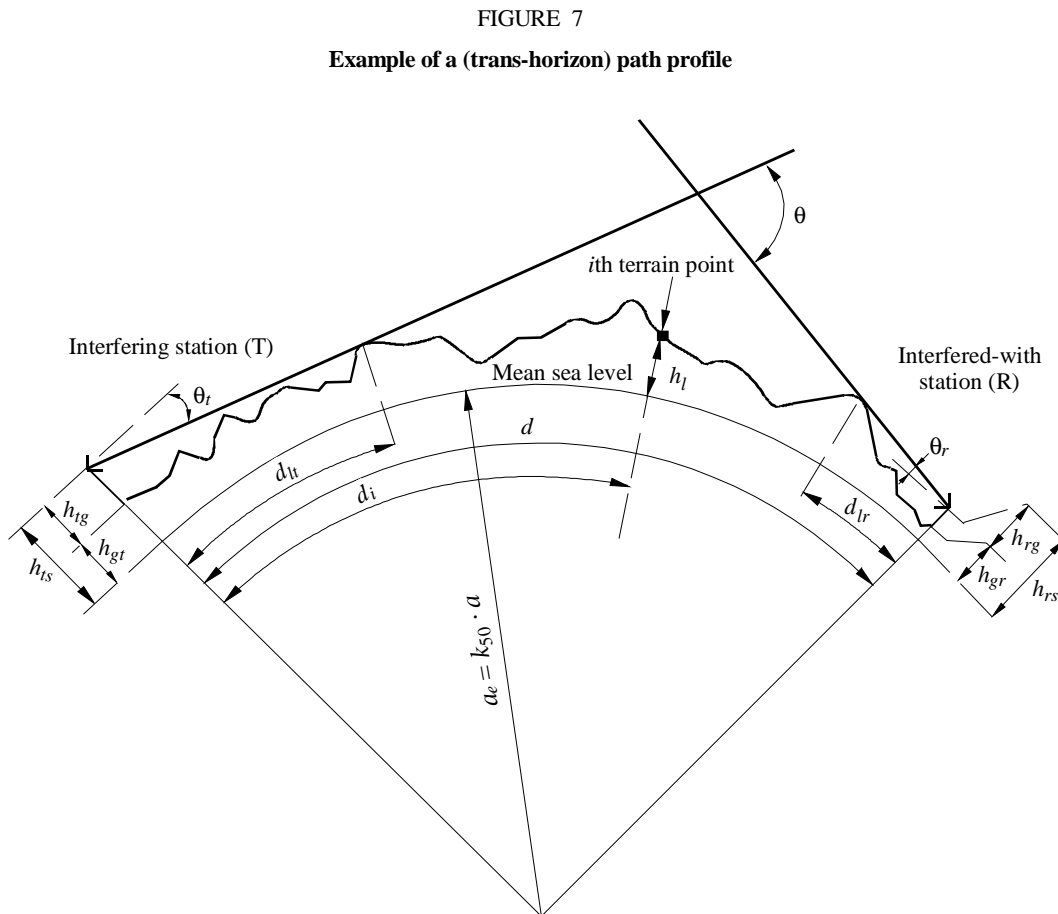
1 Introduction

For path profile analysis, a path profile of terrain heights above mean sea level is required. The parameters that need to be derived from the path profile analysis for the purposes of the propagation models are given in Table 7.

2 Construction of path profile

Based on the geographical coordinates of the interfering (ϕ_t, ψ_t) and interfered-with (ϕ_r, ψ_r) stations, terrain heights (above mean sea level) along the great-circle path should be derived from a topographical database or from appropriate large-scale contour maps. The preferred distance resolution of the profile is that giving an integer number of steps of approximately 0.25 km. Other distance increments can be used, up to a maximum of about 1 km, with some possible decrease in prediction accuracy. The profile should include the ground heights at the interfering and interfered-with station locations as the start and end points. To the heights along the path should be added the necessary Earth's curvature, based on the value of a_e found in equation (6).

For the purposes of this Recommendation the point of the path profile at the interferer is considered as point zero, and the point at the interfered-with station is considered as point n . The path profile therefore consists of $n + 1$ points. Figure 7 gives an example of a path profile of terrain heights above mean sea level, showing the various parameters related to the actual terrain.



Note 1 – The value of θ_t as drawn will be negative.

Table 7 defines parameters used or derived during the path profile analysis.

TABLE 7
Path profile parameter definitions

| Parameter | Description |
|------------|--|
| a_e | Effective Earth's radius (km) |
| d | Great-circle path distance (km) |
| d_i | Great-circle distance of the i th terrain point from the interferer (km) |
| d_{ii} | Incremental distance for regular path profile data (km) |
| f | Frequency (GHz) |
| λ | Wavelength (m) |
| h_{ts} | Interferer antenna height (m) above mean sea level (amsl) |
| h_{rs} | Interfered-with antenna height (m) (amsl) |
| θ_t | Horizon elevation angle above local horizontal (mrad), measured from the interfering antenna |
| θ_r | Horizon elevation angle above local horizontal (mrad), measured from the interfered-with antenna |
| θ | Path angular distance (mrad) |
| h_{st} | Height of the smooth-Earth surface (amsl) at the interfering station location (m) |
| h_{sr} | Height of the smooth-Earth surface (amsl) at the interfered-with station location (m) |
| h_i | Height of the i th terrain point amsl (m) NOTE 1 – h_0 : ground height of interfering station h_n : ground height of interfered-with station |
| h_m | Terrain roughness (m) |
| h_{te} | Effective height of interfering antenna (m) |
| h_{re} | Effective height of interfered-with antenna (m) |

3 Path length

For general cases the path length, d (km), can be found from the path profile data:

$$d = \sum_{i=1}^n (d_i - d_{i-1}) \quad \text{km} \quad (34)$$

however, for regularly-spaced path profile data this simplifies to:

$$d = n \cdot d_{ii} \quad \text{km} \quad (35)$$

where d_{ii} is the incremental path distance (km).

4 Path classification

The path profile must next be used to classify the path into one of three geometrical categories based on an effective Earth's radius of a_e . The interference path classifications are as indicated in Table 4.

4.1 Classification Step 1: Test for a trans-horizon path

A path is trans-horizon if the physical horizon elevation angle as seen by the interfering antenna (relative to the local horizontal) is greater than the angle (again relative to the interferer's local horizontal) subtended by the interfered-with antenna.

The test for the trans-horizon path condition is thus:

$$\theta_{max} > \theta_{td} \quad \text{mrad} \quad (36)$$

where:

$$\theta_{max} = \max_{i=1}^{n-1} (\theta_i) \quad \text{mrad} \quad (37)$$

θ_i : elevation angle to the i th terrain point

$$\theta_i = \frac{h_i - h_{ts}}{d_i} - \frac{10^3 d_i}{2 a_e} \quad \text{mrad} \quad (38)$$

where:

h_i : height of the i th terrain point (m) amsl

h_{ts} : interferer antenna height (m) amsl

d_i : distance from interferer to the i th terrain element (km)

$$\theta_{td} = \frac{h_{rs} - h_{ts}}{d} - \frac{10^3 d}{2 a_e} \quad \text{mrad} \quad (39)$$

where:

h_{rs} : interfered-with antenna height (m) amsl

d : total great-circle path distance (km)

a_e : median effective Earth's radius appropriate to the path (equation (6)).

If the condition of equation (36) is met, then the remaining path profile analysis required for trans-horizon paths can be undertaken (see § 5.1). Under these conditions step 2 of the path classification is not needed.

If the condition of equation (36) is not fulfilled, the path is line-of-sight, with or without incursion by the terrain of the first Fresnel zone.

4.2 Step 2: Test for line-of-sight with sub-path diffraction (i.e. without full first Fresnel zone clearance)

A non trans-horizon path is line-of-sight with sub-path diffraction, if the elevation angle over the physical horizon, as seen by the interfering antenna (relative to the local horizontal), and allowing for clearance equal to the first Fresnel ellipsoid radius at the horizon point, is greater than the angle (again relative to the interferer's local horizontal) subtended by the interfered-with antenna.

The path has sub-path diffraction if:

$$\theta_{fmax} > \theta_{td} \quad \text{mrad} \quad (40)$$

where:

$$\theta_{fmax} = \max_{i=1}^{n-1} (\theta_{fi}) \quad \text{mrad} \quad (41)$$

To complete this test an extra term is therefore required in equation (38) to allow for the first Fresnel ellipsoid. Recommendation ITU-R P.526, § 2, gives the radius of this ellipsoid, R_i (m), at any point along the path:

$$R_i = 17.392 \sqrt{\frac{d_i (d - d_i)}{d \cdot f}} \quad \text{m} \quad (42)$$

where f is the frequency (GHz).

The appropriate radius, R_i (m), is added to each terrain height, h_i (m), in equation (38) yielding equation (43). Allowing for first Fresnel zone clearance, θ_{fi} , the terminal antenna elevation angle (rad) to the i th point is obtained from the following equation:

$$\theta_{fi} = \frac{(h_i + R_i) - h_{ts}}{d_i} - \frac{10^3 d_i}{2 a_e} \quad \text{mrad} \quad (43)$$

If the condition of equation (40) is met, then the remaining path profile analysis required for sub-path diffraction cases can be undertaken.

If the condition of equation (40) is not fulfilled, the path is line-of-sight and no further path profile analysis is needed.

5 Derivation of parameters from the path profile

5.1 Trans-horizon paths

The parameters to be derived from the path profile are those contained in Table 7.

5.1.1 Interfering antenna horizon elevation angle, θ_t

The interfering antenna's horizon elevation angle is the maximum antenna horizon elevation angle when equation (37) is applied to the $n - 1$ terrain profile heights.

$$\theta_t = \theta_{max} \quad \text{mrad} \quad (44)$$

with θ_{max} as determined in equation (37).

5.1.2 Interfering antenna horizon distance, d_{lt}

The horizon distance is the minimum distance from the transmitter at which the maximum antenna horizon elevation angle is calculated from equation (37).

$$d_{lt} = d_i \quad \text{km} \quad \text{for max } (\theta_i) \quad (45)$$

5.1.3 Interfered-with antenna horizon elevation angle, θ_r

The receive antenna horizon elevation angle is the maximum antenna horizon elevation angle when equation (37) is applied to the $n - 1$ terrain profile heights.

$$\theta_r = \max_{j=1}^{n-1} (\theta_j) \quad \text{mrad} \quad (46)$$

$$\theta_j = \frac{h_j - h_{rs}}{d - d_j} - \frac{10^3 (d - d_j)}{2 a_e} \quad \text{mrad} \quad (47)$$

5.1.4 Interfered-with antenna horizon distance, d_{lr}

The horizon distance is the minimum distance from the receiver at which the maximum antenna horizon elevation angle is calculated from equation (37).

$$d_{lr} = d - d_j \quad \text{km} \quad \text{for max } (\theta_j) \quad (48)$$

5.1.5 Angular distance θ (mrad)

$$\theta = \frac{10^3 d}{a_e} + \theta_t + \theta_r \quad \text{mrad} \quad (49)$$

5.1.6 "Smooth-Earth" model and effective antenna heights

5.1.6.1 General

To determine the effective antenna heights, and to allow an appropriate assessment of the path roughness to be made, it is necessary to derive an effective "smooth-Earth" surface as a reference plane over which the irregular terrain of the

path is deemed to exist. Once this is derived the values of the terrain roughness parameter (§ 5.1.6.4) and effective antenna heights for the interfering and interfered-with stations can be obtained.

5.1.6.2 Exceptions

For straightforward “sea” paths, i.e. $\omega \geq 0.9$, and where both antenna horizons fall on the sea surface, the derivation of the smooth-Earth surface calculation can be omitted if required. In such case the reference plane can be taken to be a mean sea (or water) level over the whole path, the terrain roughness may be assumed to be 0 m, and the effective antenna heights are equal to the real heights above the sea surface.

For all other paths it is necessary to apply the smooth-Earth terrain approximation procedure detailed in § 5.1 and to derive the effective antenna heights and the terrain roughness as in § 5.1.6.4.

5.1.6.3 Deriving the smooth-Earth surface

Derive a straight line approximation to the terrain heights amsl of the form:

$$h_{si} = h_{st} + m \cdot d_i \quad \text{m} \quad (50)$$

where:

h_{si} : height (m) amsl, of the least-squares fit surface at distance d_i (km) from the interference source

h_{st} : height (m) amsl, of the smooth-Earth surface at the path origin, i.e. at the interfering station

m : slope (m/km) of the least-squares surface relative to sea level:

$$m = \frac{\sum_{i=0}^n (h_i - h_a) \left(d_i - \frac{d}{2} \right)}{\sum_{i=0}^n \left(d_i - \frac{d}{2} \right)^2} \quad \text{m/km} \quad (51)$$

where:

h_i : real height of the i th terrain point (m) amsl

h_a : mean of the real path heights amsl from h_0 to h_n inclusive (m):

$$h_a = \frac{1}{n+1} \sum_{i=0}^n h_i \quad \text{m} \quad (52)$$

$$h_{st} = h_a - m \frac{d}{2} \quad \text{m} \quad (53)$$

and hence the height of the smooth-Earth surface at the interfered-with station, h_{sr} , is given by:

$$h_{sr} = h_{st} + m \cdot d \quad \text{m} \quad (54)$$

Correction must then be made if the smooth-Earth heights fall above the true ground height, i.e.:

$$h_{st} = \min (h_{st}, h_0) \quad \text{m} \quad (55a)$$

$$h_{sr} = \min (h_{sr}, h_n) \quad \text{m} \quad (55b)$$

If either or both of h_{st} or h_{sr} were modified by equations (55a) or (55b) then the slope, m , of the smooth-Earth surface must also be corrected:

$$m = \frac{h_{sr} - h_{st}}{d} \quad \text{m/km} \quad (56)$$

5.1.6.4 Terrain roughness, h_m

The terrain roughness parameter, h_m (m) is the maximum height of the terrain above the smooth-Earth surface in the section of the path between, and including, the horizon points:

$$h_m = \max_{i=i_{lt}}^{i_r} [h_i - (h_{st} + m \cdot d_i)] \quad \text{m} \quad (57)$$

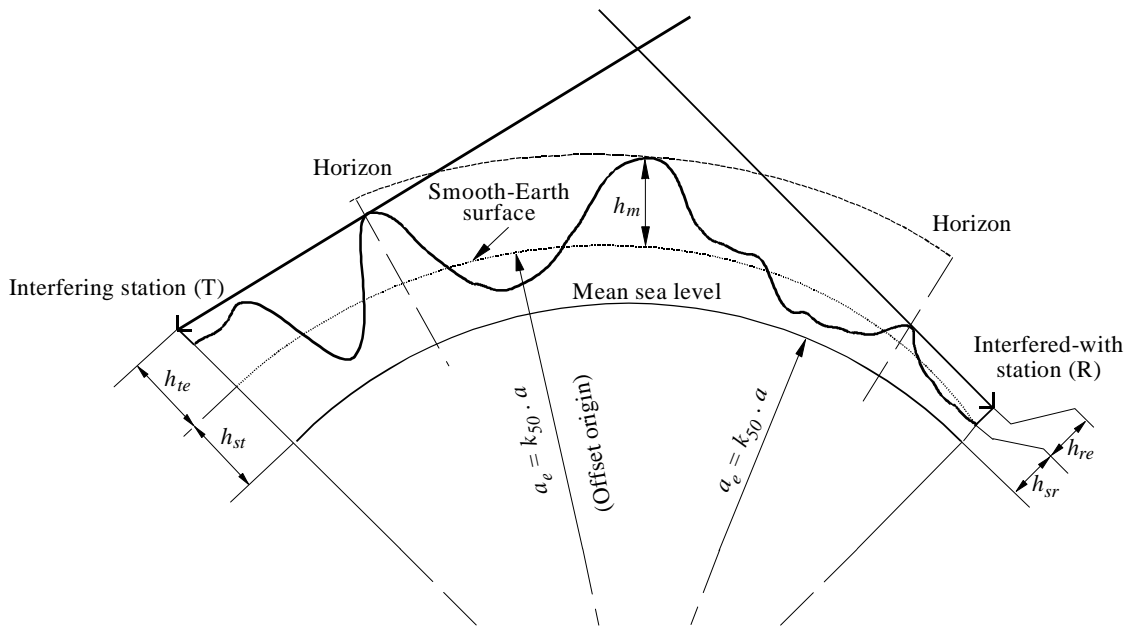
where:

i_{lt} : index of the profile point at distance d_{lt} from the transmitter

i_r : index of the profile point at distance d_{lr} from the receiver.

The smooth-Earth surface and the terrain roughness parameter h_m are illustrated in Fig. 8.

FIGURE 8
An example of the smooth-Earth surface and terrain roughness parameter



0452-08

APPENDIX 3
TO ANNEX 1

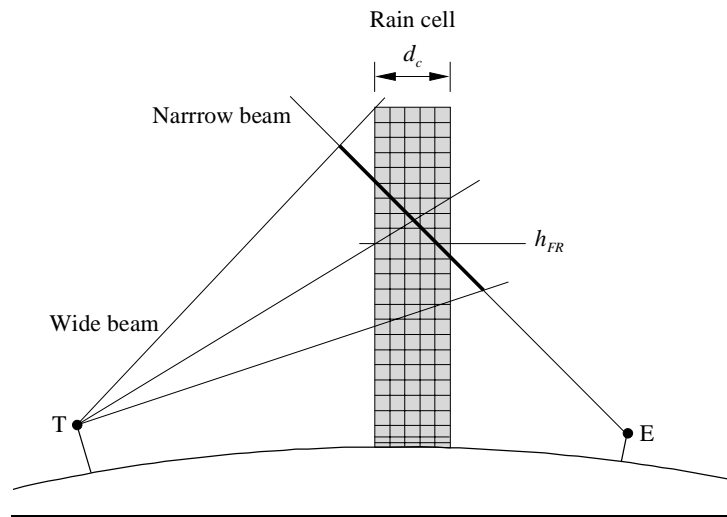
Physical basis of the hydrometeor-scatter model

Scattering is assumed to occur only within one fixed, cylindrical rain cell of circular cross-section. The diameter of the cell, d_c , depends on rainfall rate R (mm/h) as:

$$d_c = 3.3 R^{-0.08} \quad \text{km} \quad (58)$$

The cell is centred at the intersection (or point of closest approach if the beams do not exactly intersect) of the two antenna axes (see Fig. 9). This is necessary as a consequence of the inclusion of short-path geometries. Within the cell and for a given rain rate, the reflectivity is taken to be constant up to the freezing level height (or rain height), h_{FR} . Above h_{FR} it decreases at a rate of 6.5 dB/km. The rain outside the rain cell is not assumed to contribute significantly to scattering.

FIGURE 9
Rain cell position at intersection of wide beam
and narrow beam



0452-09

Rain attenuation is assumed to act only below the rain height. Inside the cell the specific attenuation, γ_R , is applied according to the formula $\gamma_R = k R^\alpha$. The coefficients k and α depend on the frequency, polarization and direction of propagation (elevation angle) of the wave and are given in Recommendation ITU-R P.838. For the attenuation, Γ_R , outside the rain cell (between the edge of the cell and a point at distance d) an exponential decrease is assumed as follows:

$$\Gamma_R = \gamma_R r_m \frac{(1 - e^{-d/r_m})}{\cos \varepsilon} \quad (59)$$

where:

r_m : scale length for rain attenuation, given by:

$$r_m = 600 R^{-0.5} 10^{-(R+1)^{0.19}} \quad \text{km} \quad (60)$$

ε : elevation angle.

Equation (59) is valid if the whole path is below the rain height. If only part of it (between distances d_1 and d_2 from the edge of the cell) is below the rain height:

$$\Gamma_R = \gamma_R r_m \frac{(e^{-d_1/r_m} - e^{-d_2/r_m})}{\cos \varepsilon} \quad (61)$$

For those portions of the propagation path that are above h_{FR} , zero rain attenuation is assumed.

Because the horizontal scale length increases rapidly with decreasing rainfall rate, the distinction between the cell and the surrounding rain will become blurred for rainfall rates below some 10 mm/h.

The rain height is treated as a random variable with a given distribution function. It is important to explicitly include the variability of the (top of) rain height, h_{FR} , in the prediction method, this being a major factor. Due to the rain attenuation acting only below h_{FR} , a common volume just above h_{FR} may result in a considerably lower transmission loss (higher

interference signal) than one below h_{FR} , despite the decrease of the reflectivity above h_{FR} . It is only in the case of a common volume sufficiently high above h_{FR} that the reflectivity decrease compensates for the absence of rain attenuation, and the transmission loss increases again. If the rain height is above the scatter volume for some part of the year and below it otherwise, the annual transmission loss statistics in the low-probability, low-loss range might be dominated by scattering from snow and ice, which would not be predicted if a fixed rain height above the scatter volume were used. This effect is more pronounced for higher frequencies, and might be negligible at frequencies below 11 GHz.

The mean value of the distribution, h_{FRm} , is taken to depend on the station's geographic latitude, ϕ (degrees). Recommendation ITU-R P.839 gives the mean value of h_{FR} .

The distribution function is given in Table 8, but locally-derived long-term values should be used if they are available.

TABLE 8
**Cumulative distributions of rain height,
 relative to the median value**

| Rain height difference (km) | Exceedence probability (%) |
|-----------------------------|----------------------------|
| -2.125 | 100.0 |
| -1.875 | 99.1 |
| -1.625 | 96.9 |
| -1.375 | 91.0 |
| -1.125 | 80.0 |
| -0.875 | 68.5 |
| -0.625 | 56.5 |
| -0.375 | 44.2 |
| -0.125 | 33.5 |
| 0.0 | 28.5 |
| 0.125 | 24.0 |
| 0.375 | 16.3 |
| 0.625 | 10.2 |
| 0.875 | 6.1 |
| 1.125 | 3.4 |
| 1.375 | 1.8 |
| 1.625 | 0.9 |

The procedure should be used with the rainfall rate distribution of the relevant rain climatic zone as given in Recommendation ITU-R P.837, unless a locally measured rainfall rate distribution is available. Each rainfall rate value will yield its own transmission loss value, which for low rainfall rates decreases with increasing rainfall rate, due to the increasing reflectivity. But for a common volume below the rain height, h_{FR} , the rain attenuation also increases with increasing rainfall rate, and will eventually outweigh the increasing reflectivity. Hence, the minimum transmission loss (on a path below h_{FR}) will be found at some intermediate rainfall rate which decreases as the frequency increases. Therefore, the conversion of the transmission loss as a function of the rainfall rate into a cumulative distribution function needs an extra step in the prediction (see § 5.3).

A "narrow-beam" approximation is used in which it is assumed that one of the antenna beams (i.e. that of the earth station) is much narrower than the other (in the vicinity of the intersection) and so, the effects of antenna gain and beamwidth cancel each other out. However, the efficiency of the narrow-beam antenna, η_E , must be included. (A default value of 0.6 is used if no value is provided.)

A Gaussian-shaped pattern for the wide-beam antenna is assumed. To account for the effect of side-lobe coupling, the side lobes of the wide-beam antenna are simulated by a second Gaussian-shaped beam which is much lower and broader

than, and is superimposed on, the main lobe. The gain of the second beam is 1 dB below the peak of the highest side lobe, and its width is so chosen that, at the position of the highest side lobe, its gain is 3 dB below that peak. In other words: gain, g^* , and (double-sided) half-power beamwidth, φ^* of the side-lobe pattern are defined by:

$$g^* = g - |\delta_g| - 1 \quad \text{dB} \quad (62)$$

$$\varphi^* = \sqrt{6} \delta \varphi = 2.45 \delta \varphi \quad (63)$$

where:

g : main-lobe axial gain (dB)

δ_g : relative gain of the highest side lobe (dB relative to g)

$\delta \varphi$: position (off-axis angle) of the highest side lobe (degrees).

The on-axis gain of the main lobe must be reduced slightly to account for the superimposed side-lobe beam, such that the sum of the two gains corresponds to the actual gain of the antenna.

Polarization coupling in equation (28) is assumed to be a maximum. In practice, rain scatter is anisotropic and the polarization of the scattered interfering signal may be different from that of the receiving antenna. The relation between these two polarizations will, in general, be complex, depending on the polarizations of the transmitting and receiving antennas, the overall geometry of the system and, to some extent, the shape of the scattering particles. If a preliminary calculation for cases of main-beam-to-main-beam coupling indicates the possibility of an interfering situation, it would in theory be possible to evaluate the coupling more precisely taking into account the above parameters.

APPENDIX 4 TO ANNEX 1

An approximation to the inverse cumulative normal distribution function for $x \leq 0.5$

The following approximation to the inverse cumulative normal distribution function is valid for $0.000001 \leq x \leq 0.5$ and is in error by a maximum of 0.00054. It may be used with confidence for the interpolation function in equation (13a). If $x < 0.000001$, which implies $\beta_0 < 0.0001\%$, x should be set to 0.000001. The function $I(x)$ is then given by:

$$I(x) = \xi(x) - T(x) \quad (67)$$

where:

$$T(x) = \sqrt{[-2 \ln(x)]} \quad (67a)$$

$$\xi(x) = \frac{[(C_2 \cdot T(x) + C_1) \cdot T(x)] + C_0}{[(D_3 \cdot T(x) + D_2) T(x) + D_1] T(x) + 1} \quad (67b)$$

$$C_0 = 2.515516698 \quad (67c)$$

$$C_1 = 0.802853 \quad (67d)$$

$$C_2 = 0.010328 \quad (67e)$$

$$D_1 = 1.432788 \quad (67f)$$

$$D_2 = 0.189269 \quad (67g)$$

$$D_3 = 0.001308 \quad (67h)$$